Eur. Phys. J. B **44**, 71–78 (2005)
DOI: 10.1140/epjb/e2005-00101-0

THE EUROPEAN PHYSICAL JOURNAL B

Theoretical calculation of the acoustic radiation force acting on elastic and viscoelastic cylinders placed in a plane standing or quasistanding wave field

F.G. Mitri[a]

Mayo Clinic College of Medicine and Foundation, Department of Physiology and Biomedical Engineering, Ultrasound Research Laboratory, 200 First Street SW, Rochester MN 55905, USA

Received 15 October 2004 / Received in final form 30 December 2004
Published online 16 April 2005 –

Abstract. In this work, a new expression of the acoustic radiation force function Y_{st} for solid cylindrical targets, suspended in inviscid fluids in a plane *standing* wave field, is presented. The case of a plane *quasistanding* wave field is also considered. Numerical calculations of the radiation force function Y_{st} are performed in a wide range of frequencies for elastic and viscoelastic cylinders and compared to those of rigid cylinders. The fluid-loading effect on the radiation force function curves is also analysed. The results show several features quite different from the rigid cylinder solution.

PACS. 43.25.+y Nonlinear acoustics – 43.20.Fn Scattering of acoustic waves

1 Introduction

The acoustic radiation force is the time-average force acting on an obstacle in a sound field, which appears in the form of a steady unidirectional force even if there is no acoustic stream. Moreover, the change in the static force occurs as a consequence of second order (nonlinear) effects of sound waves.

The problem of the acoustic radiation force acting on a sphere in a standing-wave field was initially studied by King [1]. Furthermore, various aspects of the acoustic radiation force on spheres and spherical drops were investigated [2–9].

Despite the extensive theoretical and experimental studies performed on spheres, very little work has been done to study the acoustic radiation force on cylindrically shaped structures. The first theoretical study dates back to the early work of Awatani [10] who computed the radiation force caused by progressive and stationary plane acoustic waves impinging on a rigid cylinder immersed in a compressible fluid. His calculations were performed in very limited range of frequency ($0 \leq ka \leq 5$). Later, Hasegawa et al. [11] extended his study and computed the radiation force due to progressive acoustic waves for different elastic cylinder materials. Wu et al. [12] studied experimentally the radiation force exerted by standing sound waves on a long rigid cylinder. Soon after, Hasegawa et al. [13] developed a more general theory to study the acoustic radiation force on elastic cylindrical and spherical shells.

Nevertheless, in all the previous works, sound absorption inside the cylindrical material was ignored. Recently, the theory of acoustic radiation force acting on sound-absorbing cylindrical shells [14] placed in a plane progressive sound wave field and immersed in ideal (nonviscous) fluids was investigated.

In the present paper, the theory of the acoustic radiation force experienced by solid cylinders in a plane *standing* wave field is studied. The development for the theory is useful for acoustic levitation applications in many fields such as in fluid dynamics, materials science and analytical chemistry, since the free suspension of material samples is often necessary for certain types of physical property measurements. This study follows the work done by Wei et al. [15] who studied theoretically the acoustic radiation force on a *fluid* compressible cylinder in a perfect standing wave field. However, in their approach, the radiation force was determined entirely by the scattered field at infinity (far-field approximation). In this work, an exact expression of the acoustic radiation force for *rigid*, *fluid*, *elastic* and *viscoelastic* cylinders placed in a standing plane-wave field is derived without any restriction to the near or the far-field approximation. It is shown here that the two approaches are equivalent since the cylinder is immersed in an ideal fluid. Moreover, analytical equations for a sample cylinder placed in a *quasistanding* acoustic wave field are also established. Numerical calculations are performed for different materials indicating how the radiation force can be affected by variations of the cylinder's mechanical parameters. Particular attention has been directed to sound absorption inside the viscoelastic cylinder and its effect on the acoustic radiation force. The fluid-loading effect on the radiation force function curves is analysed as well by considering a high density fluid (in this case

[a] e-mail: mitri@ieee.org

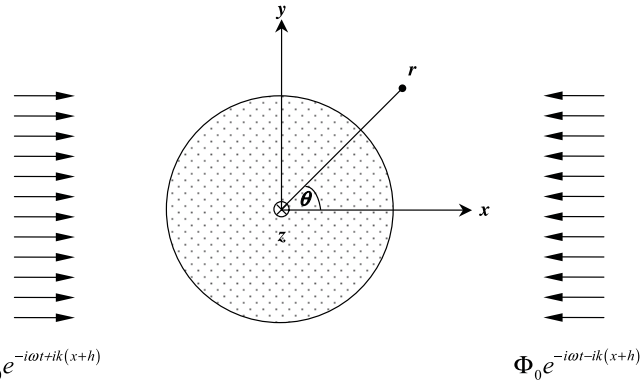

Fig. 1. 2D-frontal view of a circular cylinder placed in a plane standing wave acoustic field.

mercury) surrounding the cylinder. The analytical equations and numerical simulations show that the theory developed here is much broader in scope than previous results.

2 Method

The acoustic radiation force is commonly interpreted as the time-averaged force and it is calculated by averaging the momentum flux tensor (expressed in terms of the total pressure or velocity potential field) over the target surface and over time. It is therefore essential to calculate the total linear acoustic scattering field disturbed by the cylinder for the purpose of obtaining the radiation force.

2.1 Acoustic scattering by a solid cylinder placed in a plane standing-wave field

Consider a solid cylinder of radius a whose center is at a distance h from a pressure antinode (pressure maximum) of a plane stationary wave field at normal incidence with respect to the z-axis (Fig. 1). The cylinder is assumed to be immersed in an ideal compressible fluid, so that viscous and thermal effects can be neglected.

The incident velocity potential is expressed by

$$\Phi_{\text{inc}}^{\text{st}} = \Phi_0 e^{-i\omega t}\left\{e^{ik(x+h)} + e^{-ik(x+h)}\right\}, \tag{1}$$

where Φ_0 is the amplitude, and k is the wave number in the fluid medium.

In a system of cylindrical coordinates (r, θ, z), equation (1) can be rewritten by

$$\Phi_{\text{inc}}^{\text{st}} = \sum_{n=0}^{\infty} \Lambda_n \varepsilon_n i^n J_n(kr)\cos(n\theta)\, e^{-i\omega t}, \tag{2}$$

where $\Lambda_n = \Phi_0\left\{e^{ikh} + (-1)^n e^{-ikh}\right\}$, ε_n is the Neumann factor which is defined by $\varepsilon_0 = 1$, and $\varepsilon_j = 2$, $j = 1, \ldots n$, and $J_n(\cdot)$ is the Bessel function of the first kind of order n.

The scattered velocity potential is expressed as

$$\Phi_{\text{sc}}^{\text{st}} = \sum_{n=0}^{\infty} \Lambda_n \varepsilon_n i^n a_n H_n^{(1)}(kr)\cos(n\theta)\, e^{-i\omega t}, \tag{3}$$

where $H_n^{(1)}(\cdot)$ is the Hankel function of the first kind of order n, and a_n is the scattering coefficient to be determined from the boundary conditions. The boundary conditions are statements of continuity of stresses and displacements across the fluid-structure interface. For an elastic cylinder immersed in an ideal fluid, the following boundary conditions should be assured [16]: The displacement and normal stress must be continuous and the tangential stress must be zero.

The boundary conditions lead to three equations with three unknowns. The general solution for a_n is given by

$$a_n = \frac{\begin{vmatrix} v_1 & \lambda_{12} & \lambda_{13} \\ v_2 & \lambda_{22} & \lambda_{23} \\ v_3 & \lambda_{32} & \lambda_{33} \end{vmatrix}}{\begin{vmatrix} \lambda_{11} & \lambda_{12} & \lambda_{13} \\ \lambda_{21} & \lambda_{22} & \lambda_{23} \\ \lambda_{31} & \lambda_{32} & \lambda_{33} \end{vmatrix}}, \tag{4}$$

where λ_{ij} are the dimensionless elements of the determinants given by

$$\begin{aligned}
\lambda_{11} &= \frac{\rho}{\rho^*} x_2^2 H_n^{(1)}(x), \\
\lambda_{12} &= \left(2n^2 - x_2^2\right) J_n(x_1) - 2x_1 J_n'(x_1), \\
\lambda_{13} &= 2n\left(x_2 J_n'(x_2) - J_n(x_2)\right), \\
\lambda_{21} &= -x H_n^{(1)'}(x), \\
\lambda_{22} &= x_1 J_n'(x_1), \\
\lambda_{23} &= n J_n(x_2), \\
\lambda_{31} &= 0, \\
\lambda_{32} &= 2n\left(J_n(x_1) - x_1 J_n'(x_1)\right), \\
\lambda_{33} &= 2x_2 J_n'(x_2) - \left(2n^2 - x_2^2\right) J_n(x_2), \\
v_1 &= -\frac{\rho}{\rho^*} x_2^2 J_n(x), \\
v_2 &= x J_n'(x), \\
v_3 &= 0,
\end{aligned}$$

where ρ and ρ^* are the mass densities of the fluid and elastic medium, respectively, $x = ka$, and is defined as the dimensionless size parameter, where $k = \frac{\omega}{c}$ and c is the sound velocity in the fluid medium, $x_1 = x\frac{c}{c_1}$ and $x_2 = x\frac{c}{c_2}$ where c_1 and c_2 are the compressional and shear wave velocities in the cylinder. Here and elsewhere the primes denote derivatives with respect to the arguments.

The term a_n is a complex number that can be written as

$$a_n = (\alpha_n + i\beta_n). \tag{5}$$

Thus, the total (incident + scattered) velocity potential is expressed by

$$\Phi_{\text{t}}^{\text{st}} = \sum_{n=0}^{\infty} \Lambda_n \varepsilon_n i^n (U_n + iV_n)\cos(n\theta)\, e^{-i\omega t}, \tag{6}$$

where U_n and V_n are given by the following equations:

$$U_n = (1+\alpha_n) J_n(kr) - \beta_n Y_n(kr),$$
$$V_n = \beta_n J_n(kr) + \alpha_n Y_n(kr). \quad (7)$$

2.2 Acoustic radiation force on a solid cylinder placed in a plane standing-wave field

The total averaged-force caused by acoustic waves on a cylinder's boundary moving at a velocity of the first order in the amplitude of the incident acoustic field is expressed by [3]

$$\langle F\rangle = -\iint_S \left[\left(\frac{1}{2}\frac{\rho}{c^2}\left\langle\left(\frac{\partial \Psi^{\rm st}}{\partial t}\right)^2\right\rangle - \frac{1}{2}\rho\left\langle\left|\nabla\Psi^{\rm st}\right|^2\right\rangle\right)\mathbf{n} + \rho\left\langle\left(v_n\mathbf{n}+v_t\mathbf{t}\right)v_n\right\rangle\right] dS, \quad (8)$$

where S is the surface of the cylinder at its *equilibrium* position, and

$$\Psi^{\rm st} = {\rm Re}[\Phi_{\rm t}^{\rm st}] = \sum_{n=0}^{\infty} \varepsilon_n R_n \cos(n\theta), \quad (9)$$

in which the functions $R_n = {\rm Re}[(i)^n (U_n(kr) + iV_n(kr))\Lambda_n e^{-i\omega t}]$, and $-\nabla\Psi^{\rm st}$ is the first order fluid particle velocity of the boundary, and $\Phi_{\rm t}^{\rm st}$ is the total velocity potential in the fluid medium described in equation (6). $v_n\mathbf{n}$ and $v_t\mathbf{t}$ are the normal and tangential components of the particle velocity of the boundary, respectively.

In the direction of wave propagation (x-direction), the radiation force per unit-length of the cylinder is expressed as [11]

$$\langle F_x\rangle = \langle F_r\rangle + \langle F_\theta\rangle + \langle F_{r\theta}\rangle + \langle F_t\rangle, \quad (10)$$

where

$$\langle F_r\rangle = \left\langle -\frac{1}{2}a\rho\int_0^{2\pi}\left(\frac{\partial\Psi^{\rm st}}{\partial r}\right)^2_{r=a}\cos\theta\, d\theta\right\rangle,$$
$$\langle F_\theta\rangle = \left\langle \frac{1}{2a}\rho\int_0^{2\pi}\left(\frac{\partial\Psi^{\rm st}}{\partial \theta}\right)^2_{r=a}\cos\theta\, d\theta\right\rangle,$$
$$\langle F_{r\theta}\rangle = \left\langle \rho\int_0^{2\pi}\left(\frac{\partial\Psi^{\rm st}}{\partial r}\right)_{r=a}\left(\frac{\partial\Psi^{\rm st}}{\partial \theta}\right)_{r=a}\sin\theta d\theta\right\rangle,$$
$$\langle F_t\rangle = \left\langle -\frac{1}{2c^2}a\rho\int_0^{2\pi}\left(\frac{\partial\Psi^{\rm st}}{\partial t}\right)^2_{r=a}\cos\theta\, d\theta\right\rangle. \quad (11)$$

The functions R_n satisfy the following relations:

$$\langle R_n R_{n+1}\rangle = (-1)^{n+1}|\Phi_0|^2 (U_n U_{n+1} + V_n V_{n+1})\sin(2kh),$$
$$\langle R'_n R'_{n+1}\rangle = (-1)^{n+1}|\Phi_0|^2 (U'_n U'_{n+1} + V'_n V'_{n+1})\sin(2kh),$$
$$\langle R_n R'_{n+1}\rangle = (-1)^{n+1}|\Phi_0|^2 (U_n U'_{n+1} + V_n V'_{n+1})\sin(2kh),$$
$$\langle R'_n R_{n+1}\rangle = (-1)^{n+1}|\Phi_0|^2 (U'_n U_{n+1} + V'_n V_{n+1})\sin(2kh),$$
$$\left\langle \frac{\partial R_n}{\partial t}\cdot\frac{\partial R_{n+1}}{\partial t}\right\rangle = \omega^2\langle R_n R_{n+1}\rangle, \quad (12)$$

so that equation (10) can be rewritten in another form using equations (11);

$$\begin{aligned}
\langle F_r\rangle &= -2\pi a\rho\sum_{n=0}^{\infty}\langle R'_n R'_{n+1}\rangle|_{r=a}\\
&= -\frac{2x^2\pi\rho|\Phi_0|^2}{a}\sum_{n=0}^{\infty}(-1)^{n+1}\\
&\quad\times\left(U'_n U'_{n+1} + V'_n V'_{n+1}\right)\sin(2kh),\\
\langle F_\theta\rangle &= \frac{2\pi\rho}{a}\sum_{n=0}^{\infty} n(n+1)\langle R_n R_{n+1}\rangle\\
&= \frac{2\pi\rho|\Phi_0|^2}{a}\sum_{n=0}^{\infty} n(n+1)(-1)^{n+1}\\
&\quad\times(U_n U_{n+1} + V_n V_{n+1})\sin(2kh),\\
\langle F_{r,\theta}\rangle &= 2\pi\rho\sum_{n=0}^{\infty}\left[n\langle R_n R'_{n+1}\rangle\big|_{r=a} - (n+1)\right.\\
&\quad\left.\times\langle R'_n R_{n+1}\rangle\big|_{r=a}\right]\\
&= \frac{2x\pi\rho|\Phi_0|^2}{a}\sum_{n=0}^{\infty}(-1)^{n+1}\\
&\quad\times\left[n\left(U_n U'_{n+1} + V_n V'_{n+1}\right) - (n+1)\right.\\
&\quad\left.\times(U'_n U_{n+1} + V'_n V_{n+1})\right]\sin(2kh),\\
\langle F_t\rangle &= -\frac{2\pi a\rho}{c^2}\sum_{n=0}^{\infty}\left\langle\frac{\partial R_n}{\partial t}\cdot\frac{\partial R_{n+1}}{\partial t}\right\rangle\\
&= -\frac{2x^2\pi\rho|\Phi_0|^2}{a}\sum_{n=0}^{\infty}(-1)^{n+1}\\
&\quad\times(U_n U_{n+1} + V_n V_{n+1})\sin(2kh). \quad (13)
\end{aligned}$$

If we denote by $\langle E_p\rangle = \frac{1}{2}\rho k^2|\Phi_0|^2$ the mean energy density of the incident *progressive* plane wave (where its velocity potential is given by $\Phi_{\rm inc}^{\rm p} = \Phi_0 e^{-i(\omega t - kx)}$), and replace equations (7) in equations (13), substitute them into equation (10), and after some manipulation, the final expression of the radiation force (per unit-length) can be greatly simplified and is given by

$$\langle F_x\rangle_{st} = Y_{st} S_c \langle E_p\rangle \sin(2kh). \quad (14)$$

In equation (14), $S_c = 2a$ is the cross-sectional area for a *unit-length* cylinder, and Y_{st} is a dimensionless factor (called the radiation force function for standing waves) that depends on the scattering and absorption properties of the target. Y_{st} is the radiation force per unit cross section and unit energy density expressed by

$$Y_{st} = \frac{4}{x}\sum_{n=0}^{\infty}(-1)^{n+1}\left[\beta_n(1+2\alpha_{n+1}) - \beta_{n+1}(1+2\alpha_n)\right]. \quad (15)$$

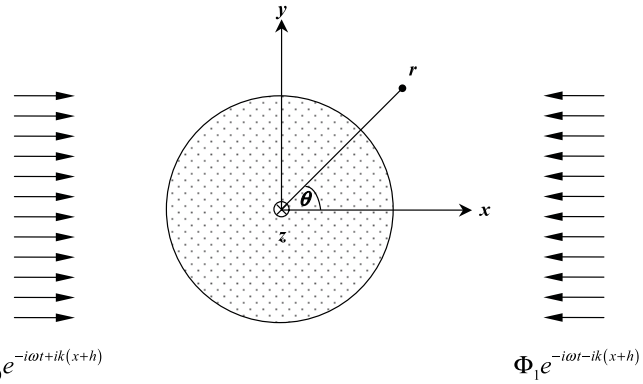

Fig. 2. 2D-frontal view of a circular cylinder placed in a partial or quasistanding wave acoustic field.

2.3 Acoustic radiation force on a solid cylinder placed in a plane quasistanding wave field

In the previous section, the acoustic radiation force acting on solid cylinders in a perfect standing plane-wave field was calculated. The cylinder's axis was constrained to be parallel to the equi-amplitude plane standing waves incident from both directions ($\theta = 0$ and $\theta = \pi$) (Fig. 1).

In this section, the acoustic radiation force resulting from a quasistanding plane-wave field will be analyzed.

In a quasistanding-wave field (Fig. 2), the incident velocity potential is expressed by

$$\Phi_{\text{inc}}^{\text{qs}} = e^{-i\omega t}\left\{\Phi_0 e^{ik(x+h)} + \Phi_1 e^{-ik(x+h)}\right\}, \tag{16}$$

with the assumption that $\Phi_0 > \Phi_1$.

In the cylindrical coordinates, the total velocity potential can be expressed by

$$\Phi_{\text{t}}^{\text{qs}} = \sum_{n=0}^{\infty} \Omega_n \varepsilon_n i^n \left(U_n + iV_n\right)\cos\left(n\theta\right) e^{-i\omega t}, \tag{17}$$

where $\Omega_n = \Phi_0 e^{ikh} + (-1)^n \Phi_1 e^{-ikh}$ and the functions $R_n = \text{Re}[(i)^n (U_n(kr) + iV_n(kr))\Omega_n e^{-i\omega t}]$.

The expressions corresponding to equations (12) become as follows,

$$\begin{aligned}
\langle R_n R_{n+1}\rangle &= (-1)^{n+1}\left|\Phi_0\right|\left|\Phi_1\right|\left(U_n U_{n+1} + V_n V_{n+1}\right)\\
&\quad\times \sin(2kh) + \frac{\left|\Phi_0\right|^2 - \left|\Phi_1\right|^2}{2}\left(U_n V_{n+1} - V_n U_{n+1}\right),\\
\left\langle R'_n R'_{n+1}\right\rangle &= (-1)^{n+1}\left|\Phi_0\right|\left|\Phi_1\right|\left(U'_n U'_{n+1} + V'_n V'_{n+1}\right)\\
&\quad\times \sin(2kh) + \frac{\left|\Phi_0\right|^2 - \left|\Phi_1\right|^2}{2}\left(U'_n V'_{n+1} - V'_n U'_{n+1}\right),\\
\left\langle R_n R'_{n+1}\right\rangle &= (-1)^{n+1}\left|\Phi_0\right|\left|\Phi_1\right|\left(U_n U'_{n+1} + V_n V'_{n+1}\right)\\
&\quad\times \sin(2kh) + \frac{\left|\Phi_0\right|^2 - \left|\Phi_1\right|^2}{2}\left(U_n V'_{n+1} - V_n U'_{n+1}\right),\\
\langle R'_n R_{n+1}\rangle &= (-1)^{n+1}\left|\Phi_0\right|\left|\Phi_1\right|\left(U'_n U_{n+1} + V'_n V_{n+1}\right)\\
&\quad\times \sin(2kh) + \frac{\left|\Phi_0\right|^2 - \left|\Phi_1\right|^2}{2}\left(U'_n V_{n+1} - V'_n U_{n+1}\right),\\
\left\langle \frac{\partial R_n}{\partial t}\cdot\frac{\partial R_{n+1}}{\partial t}\right\rangle &= \omega^2\left\langle R_n R_{n+1}\right\rangle.
\end{aligned} \tag{18}$$

By using equations (18), we obtain in correspondence with equations (13) the following formulas:

$$\begin{aligned}
\langle F_r\rangle &= -\frac{2x^2\pi\rho}{a}\sum_{n=0}^{\infty}\Bigg\{(-1)^{n+1}\left|\Phi_0\right|\left|\Phi_1\right|\\
&\quad\times\left(U'_n U'_{n+1} + V'_n V'_{n+1}\right)\sin(2kh)\\
&\quad+\frac{\left|\Phi_0\right|^2 - \left|\Phi_1\right|^2}{2}\left(U'_n V'_{n+1} - V'_n U'_{n+1}\right)\Bigg\},\\
\langle F_\theta\rangle &= \frac{2\pi\rho}{a}\sum_{n=0}^{\infty} n\left(n+1\right)\Bigg\{(-1)^{n+1}\left|\Phi_0\right|\left|\Phi_1\right|\\
&\quad\times\left(U_n U_{n+1} + V_n V_{n+1}\right)\sin(2kh)\\
&\quad+\frac{\left|\Phi_0\right|^2 - \left|\Phi_1\right|^2}{2}\left(U_n V_{n+1} - V_n U_{n+1}\right)\Bigg\},
\end{aligned}$$

$$\begin{aligned}
\langle F_{r,\theta}\rangle &= \frac{2x\pi\rho}{a}\\
&\quad\times\sum_{n=0}^{\infty}\left\{\begin{array}{l}(-1)^{n+1}\left|\Phi_0\right|\left|\Phi_1\right|\left[n\left(U_n U'_{n+1} + V_n V'_{n+1}\right)\right.\\ -(n+1)\left(U'_n U_{n+1} + V'_n V_{n+1}\right)]\sin(2kh)\\ +\frac{\left|\Phi_0\right|^2-\left|\Phi_1\right|^2}{2}\left[n\left(U_n V'_{n+1} - V_n U'_{n+1}\right)\right.\\ -(n+1)\left(U'_n V_{n+1} - V'_n U_{n+1}\right)]\end{array}\right\},
\end{aligned}$$

$$\begin{aligned}
\langle F_t\rangle &= -\frac{2x^2\pi\rho}{a}\sum_{n=0}^{\infty}\Bigg\{(-1)^{n+1}\left|\Phi_0\right|\left|\Phi_1\right|\\
&\quad\times\left(U_n U_{n+1} + V_n V_{n+1}\right)\sin(2kh)\\
&\quad+\frac{\left|\Phi_0\right|^2 - \left|\Phi_1\right|^2}{2}\left(U_n V_{n+1} - V_n U_{n+1}\right)\Bigg\}.
\end{aligned} \tag{19}$$

The quasistationary radiation force is identical to equation (10) and is given by

$$\langle F_x\rangle_{qs} = Y_{qs} S_c \langle E_p\rangle, \tag{20}$$

where $\langle E_p\rangle$ is being defined previously in Section 2.2, and Y_{qs} is expressed by

$$\begin{aligned}
Y_{qs} &=\\
&\frac{4}{x}\sum_{n=0}^{\infty}\left\{\begin{array}{l}(-1)^{n+1}\,\frac{\left|\Phi_1\right|}{\left|\Phi_0\right|}\left[\beta_n\left(1+2\alpha_{n+1}\right)\right.\\ \quad-\beta_{n+1}\left(1+2\alpha_n\right)]\sin\left(2kh\right)\\ -\left(\frac{\left|\Phi_0\right|^2-\left|\Phi_1\right|^2}{2\left|\Phi_0\right|^2}\right)\\ \quad\times\left[\alpha_n+\alpha_{n+1}+2\left(\alpha_n\alpha_{n+1}+\beta_n\beta_{n+1}\right)\right]\end{array}\right\}.
\end{aligned} \tag{21}$$

Moreover, Hasegawa et al. [11] introduced the radiation force function for plane progressive sound waves, which is given by

$$\begin{aligned}
Y_p &= \frac{\langle F_x\rangle_p}{S_c\langle E_p\rangle}\\
&= -\frac{2}{x}\sum_{n=0}^{\infty}\left[\alpha_n+\alpha_{n+1}+2\left(\alpha_n\alpha_{n+1}+\beta_n\beta_{n+1}\right)\right].
\end{aligned} \tag{22}$$

Table 1. Material parameters used in the numerical calculations.

Material	Mass density [10^3 kg/m^3]	Compressional Velocity [m/s]	Shear Velocity [m/s]	Normalized longitudinal absorption γ_1	Normalized shear absorption γ_2
Air	0.00123	340	...	...	...
Brass	8.1	3830	2050	...	...
Gold	19.3	3240	1200	...	...
Lucite	1.191	2690	1340	0.0035	0.0053
Mercury	13.6	1407	...	...	...
Phenolic polymer	1.22	2840	1320	0.0119	0.0257
Water	1.00	1500	...	...	...

Hence, the radiation force function for quasistationary waves can be expressed by terms of the radiation force function for progressive and standing waves. By substituting equations (15) and (22) into equation (21), the radiation force function for quasistationary waves is now expressed as

$$Y_{qs} = Y_p \left\{ \left(1 - \frac{|\Phi_1|^2}{|\Phi_0|^2} \right) + \frac{|\Phi_1|}{|\Phi_0|} \frac{Y_{st}}{Y_p} \sin(2kh) \right\} \qquad (23)$$

and hence, the radiation force is

$$\begin{aligned} \langle F_x \rangle_{qs} &= \left(1 - \frac{|\Phi_1|^2}{|\Phi_0|^2} \right) \langle F_x \rangle_p + \frac{|\Phi_1|}{|\Phi_0|} \langle F_x \rangle_{st} \\ &= \langle F_x \rangle_p \left\{ \left(1 - \frac{|\Phi_1|^2}{|\Phi_0|^2} \right) + \frac{|\Phi_1|}{|\Phi_0|} \frac{Y_{st}}{Y_p} \sin(2kh) \right\}. \end{aligned} \qquad (24)$$

Equation (24) is the general formula for the radiation force for any quasistationary field with known $|\Phi_0|$ and $|\Phi_1|$. It can be easily verified that when $|\Phi_1| = 0$, Y_{qs} is reduced to the radiation force function for a plane progressive wave-field, and when $|\Phi_0| = |\Phi_1|$, Y_{qs} is equivalent to the radiation force function for a stationary wave-field. Moreover, the magnitude of $\langle F_x \rangle_{qs}$ varies periodically as a function of the position of the cylinder; the spatial mean value of $\langle F_x \rangle_{qs}$ is equal to $\left(1 - \frac{|\Phi_1|^2}{|\Phi_0|^2} \right) \langle F_x \rangle_p$.

3 Numerical results and discussion

3.1 Compressible fluid cylinder

As an initial test, the results obtained by Wei et al. [15] for fluid cylinders were recalculated. Equation (15) was used to compute the acoustic radiation force function Y_{st}. Figure 3 shows the radiation force function for a water cylinder surrounded by air (see Tab. 1) in a standing wave field that will be compared to Figure 3 in the paper of Wei et al. [15]; perfect agreement was found. The results for the fluid cylinder were obtained using the adequate scattering coefficients defined in equation (4) by allowing the shear wave velocity c_2 tending to zero.

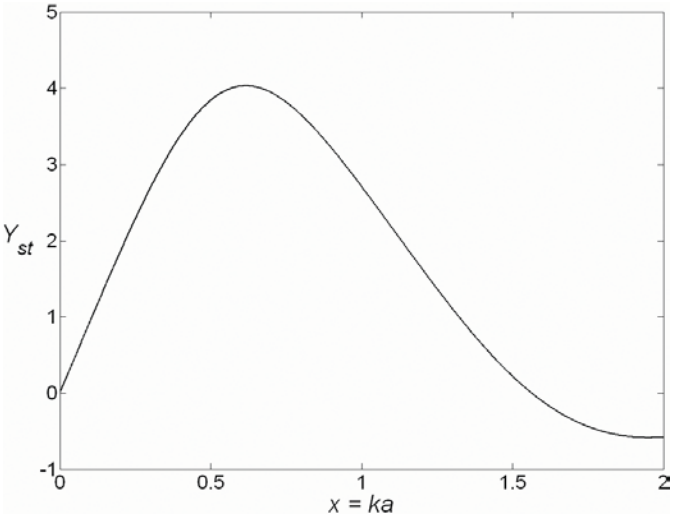

Fig. 3. Y_{st} curve for a water cylinder in air in a standing wave.

3.2 Rigid and elastic cylinders

The calculations for rigid and elastic cylinders in a standing-wave field were performed using equation (15) for brass material as an example. The cylinders were assumed to be immersed in water. The mechanical parameters of brass used in the calculations are listed in Table 1.

The radiation force function Y_{st} curves were plotted as a function of the size parameter $x = ka$, (a being the cylinder's radius) in a large range of frequency defined by $0 \leq x \leq 60$ in intervals of 0.01. It is very important to choose a sufficiently small sampling step since resonance peaks are very sharp and a wrong sampling may lead to false curves. It was also verified that the Y_{st} curves do not vary significantly when the step value is decreased.

For brass cylinders, the scattering coefficients defined by equation (4) were used, whereas for rigid cylinders, these scattering coefficients were reduced to $a_n = \frac{v_2}{\lambda_{21}}$. Figure 4 shows a comparison between the Y_{st} curves for rigid and elastic brass cylinders immersed in water. One notices the great change between the rigid and elastic cylinder solutions. However, the change is less prominent between the curves for approximately $x = ka < 1$. For elastic materials, resonance peaks do appear at high ka values.

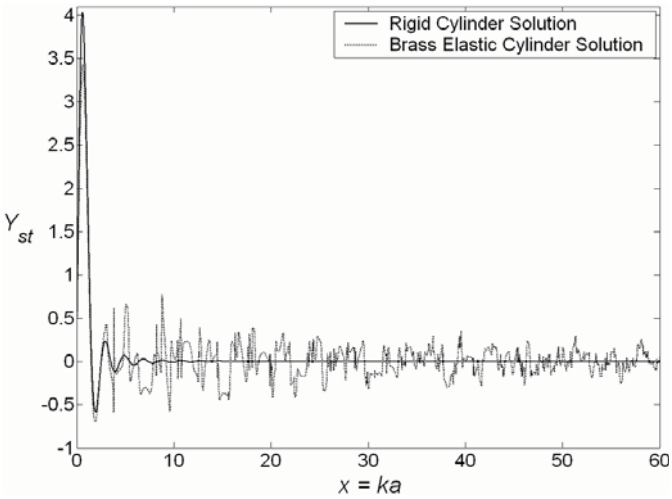

Fig. 4. Comparison of the Y_{st} curves for rigid and brass elastic cylinders immersed in water in a standing wave. One notices the great change between the rigid and elastic solutions. With elastic materials, successive maxima and minima peaks tend to appear for high ka values.

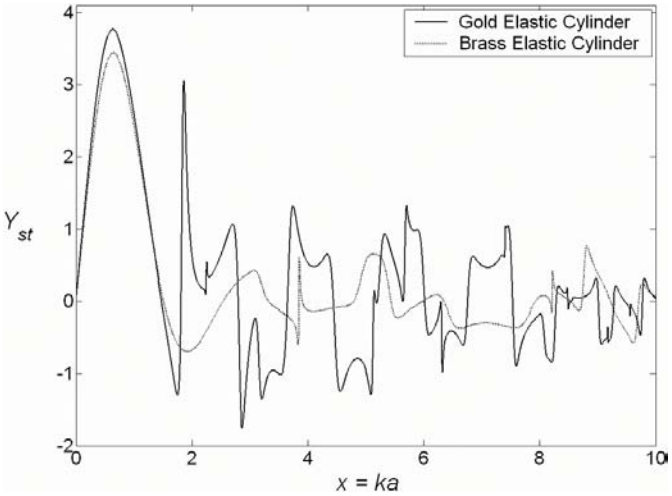

Fig. 5. Comparison of the Y_{st} curves for brass and gold elastic cylinders immersed in water in a standing wave. One notices that the radiation force function Y_{st} is higher for heavier materials.

Figure 5 shows additional computation of the Y_{st} curves for brass and gold (heavier than brass) (Tab. 1) elastic cylinders immersed in water in the range $0 \leq x \leq 10$. It is obvious that radiation force for the gold cylinder is greater than for brass. In addition, both materials are heavier than the propagation medium so that the cylinders are attracted to a pressure node ($Y_{st} > 0$) in the low frequency range; $0 \leq x \leq 1.5$.

Cylinders are predicted to be attracted to pressure nodes when $Y_{st} > 0$ and to pressure antinodes when $Y_{st} < 0$, and the radiation force vanishes for $kh = \pm\frac{n\pi}{2}$ (Eq. (14)). If the cylinder is centered on a pressure antinode, $n = 0$, and if it is centered on a pressure node $n = 1, 2, ...$ The magnitude of the radiation force is maximal when the cylinder is at the intermediate location defined by $kh = \pm\,(2n+1)\,\frac{\pi}{4}, n = 0, 1...$

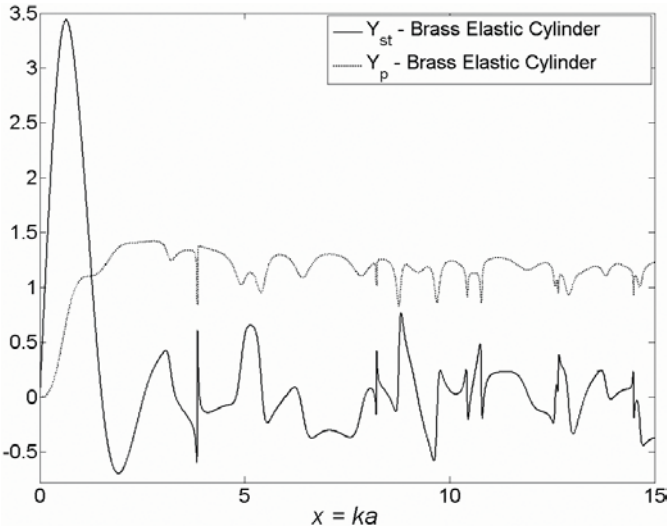

Fig. 6. Comparison between the Y_{st} and Y_p curves for a brass elastic cylinder. Obviously, resonance peaks appear at the same ka values.

3.3 Comparison of the radiation force functions for plane progressive and standing wave fields for an elastic cylinder

Additional calculations were performed in order to compare the acoustic radiation force functions Y_p (Eq. (22)) and Y_{st} (Eq. (15)) for progressive and standing waves incident upon an elastic brass cylinder.

Figure 6 shows the combined calculations of the progressive and standing wave acoustic radiation force functions for a brass cylinder immersed in water in the range $0 \leq x \leq 15$. The peaks in both curves correspond to resonance frequencies of the elastic cylinder. These resonances are directly linked to the resonance vibrational modes. One notices that the position of the resonance peaks in the radiation force function curves for both progressive and standing wave configurations correlate well. However, dips or minima in the Y_p curves appear as maxima in the Y_{st} curves. A detailed discussion on whether the resonances are manifested as either maxima or minima in the radiation force function curves is very subtle [17] and is beyond of the scope of this work. Further studies should seek to identify each factor that contributes to the acoustic radiation force separately in order to address that question.

3.4 Viscoelastic cylinders

Numerical calculations for viscoelastic lucite and phenolic polymer cylinders were evaluated using equation (15). Absorption of sound inside the viscoelastic material was included by introducing complex size parameters into the theory [18] such as $\tilde{x}_1 = x_1\,(1 + i\gamma_1)$ and

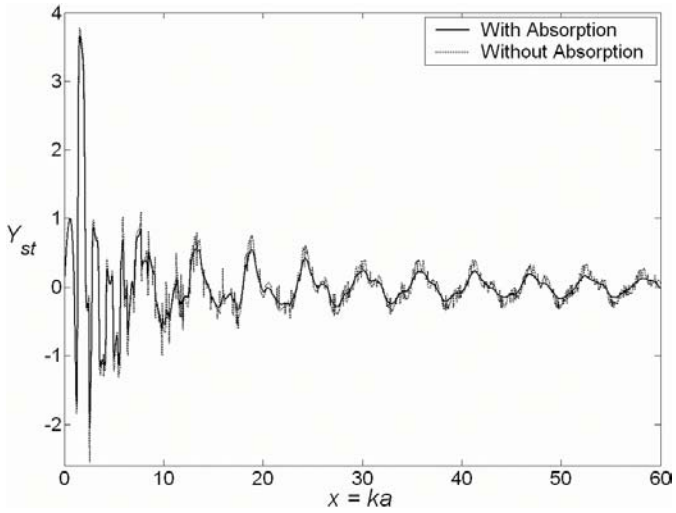

Fig. 7. Y_{st} curves for a lucite cylinder immersed in water in a standing wave with and without absorption.

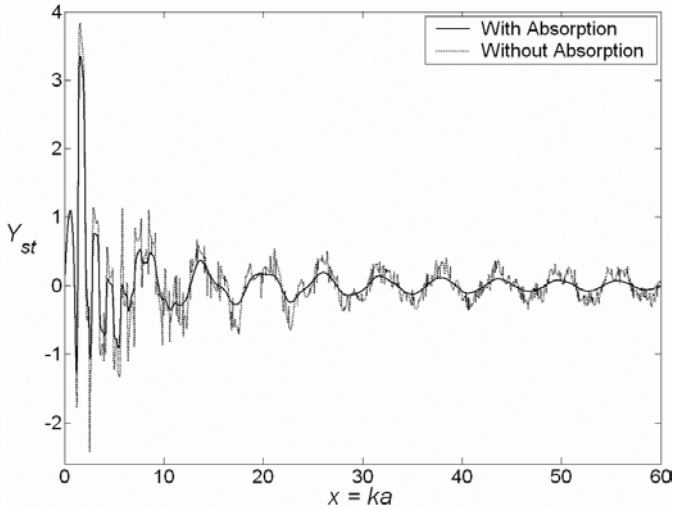

Fig. 8. Same as Figure 7 but for a phenolic polymer cylinder. The damping of resonance peaks appear more clearly for this material whose normalized absorption coefficients are greater than lucite.

$\tilde{x}_2 = x_2\,(1 + i\gamma_2)$, where γ_1 and γ_2 are the normalized absorption coefficients of the compressional and shear wave velocities, respectively. Table 1 lists the mechanical parameters of these materials used in the simulations. The Y_{st} curves were plotted in the same range of frequency as mentioned in Section 3.2.

Figures 7 and 8 show the acoustic radiation force function for lucite and phenolic polymer cylinders, respectively, with and without absorption. Notice that the damping of all peaks appears more clearly for the phenolic polymer material (Fig. 8) whose normalized absorption coefficients are greater than lucite.

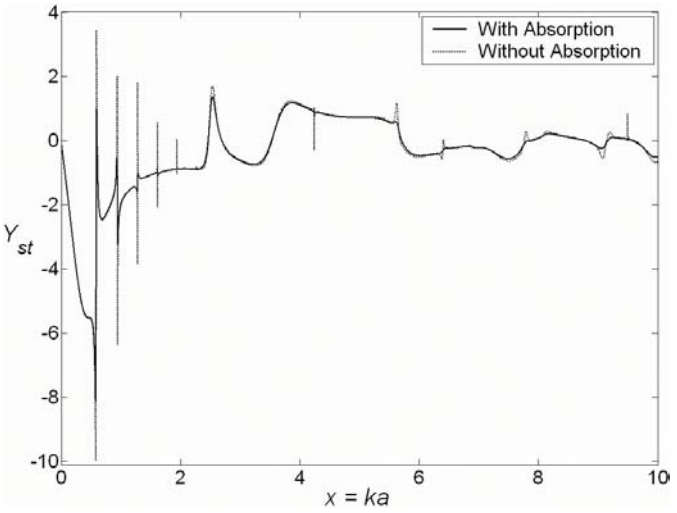

Fig. 9. Y_{st} curves for a lucite cylinder immersed in mercury in a standing wave with and without absorption. The fluid-loading has a significant impact on the Y_{st} curves; a high resonance minima peak appears clearly at low frequency ($ka = 0.58$). Furthermore, the acoustic radiation force is not greatly affected by sound absorption inside the viscoelastic material when immersed in a high density fluid.

3.5 Solid cylinder in a high density fluid

Figure 9 shows additional calculations of the acoustic radiation force function Y_{st} for lucite cylinders immersed in mercury in the range $0 \leq x \leq 10$ with and without absorption. Obviously, the fluid-loading effect on the radiation force function curves is significant. The fluid-loading produces interactions between various resonance vibrational modes that can have a significant impact on radiation force. This is clearly observed in Figure 9 where a "giant resonance peak" appears at low frequency ($x = ka = 0.58$).

A similar behavior was observed in the radiation force function for progressive waves [14] and in the acoustic backscattering form function of viscoelastic cylinders immersed in a high density fluid [18]. It is clearly shown from this figure that the cylinder, lighter than the propagation medium (mercury), is attracted to a pressure antinode ($Y_{st} < 0$) in the low frequency region. Moreover, for high density fluids, the radiation force is not greatly affected by sound absorption in the viscoelastic cylinder.

4 Conclusion

In this work, an exact expression for the acoustic radiation force experienced by fluid, rigid, elastic and viscoelastic cylinders immersed in ideal fluids and placed in a standing or quasistanding wave field is developed. Analytical equations are derived and numerical calculations of the radiation force function Y_{st} are performed for different materials. Particular emphasis is focused on the effect of sound absorption by the viscoelastic cylinders, and the surrounding fluid. The results indicate the ways in which

the radiation force function curves are affected by variations in the cylinder mechanical properties. For rigid cylinders, the results show significant changes from the elastic cylinder solutions in which successive maxima and minima tend to appear pronounced in the high $x(=ka)$ region.

References

1. L.V. King, Proc. R. Soc. London Ser. A **147**, 212 (1935)
2. T.F.W. Embleton, J. Acoust. Soc. Am. **26**, 40 (1954)
3. K. Yosioka, Y. Kawasima, Acustica **5**, 167 (1955)
4. G. Maindanik, P.J. Westervelt, J. Acoust. Soc. Am. **29**, 936 (1957)
5. L.P. Gor'kov, Sov. Phys. Dokl. **6**, 773 (1962)
6. W.L. Nyborg, J. Acoust. Soc. Am. **42**, 947 (1967)
7. L.A. Crum, J. Acoust. Soc. Am. **50**, 157 (1971)
8. T. Hasegawa, J. Acoust. Soc. Am. **65**, 32 (1979)
9. A.A. Doinikov, J. Acoust. Soc. Am. **101**, 713 (1997)
10. J. Awatani, Mem. Inst. Sci. Ind. Osaka Univ. **12**, 95 (1955)
11. T. Hasegawa, K. Saka, N. Inoue, K. Matsuzawa, J. Acoust. Soc. Am. **83**, 1770 (1988)
12. J. Wu, G. Du, S.S. Work, D.M. Warshaw, J. Acoust. Soc. Am. **87**, 581 (1990)
13. T. Hasegawa, Y. Hino, A. Annou, H. Noda, M. Kato, J. Acoust. Soc. Am. **93**, 154 (1993)
14. F.G. Mitri, Ultrasonics **43**, 271 (2005)
15. W. Wei, D.B. Thiessen, P.L. Marston, J. Acoust. Soc. Am. **116**, 201 (2004)
16. J.J. Faran, J. Acoust. Soc. Am. **23**, 405 (1951)
17. F.G. Mitri, S. Chen, Phys. Rev. E **71**, 016306 (2005)
18. F.G. Mitri, Z.E.A. Fellah, J.Y. Chapelon, J. Acoust. Soc. Am. **115**, 1411 (2004)